



HAL
open science

Development of NH₃/H₂O absorption chillers for negative cooling in industrial solar systems.

Hélène Demasles, Anouk Muller, Hai Trieu Phan

► To cite this version:

Hélène Demasles, Anouk Muller, Hai Trieu Phan. Development of NH₃/H₂O absorption chillers for negative cooling in industrial solar systems.. 26th International Congress of Refrigeration, Aug 2023, Paris, France. 10.18462/iir.icr.2023.0054 . hal-04314918

HAL Id: hal-04314918

<https://hal.science/hal-04314918>

Submitted on 5 Dec 2023

HAL is a multi-disciplinary open access archive for the deposit and dissemination of scientific research documents, whether they are published or not. The documents may come from teaching and research institutions in France or abroad, or from public or private research centers.

L'archive ouverte pluridisciplinaire **HAL**, est destinée au dépôt et à la diffusion de documents scientifiques de niveau recherche, publiés ou non, émanant des établissements d'enseignement et de recherche français ou étrangers, des laboratoires publics ou privés.

Public Domain

DEVELOPMENT OF NH₃/H₂O ABSORPTION CHILLERS FOR NEGATIVE COOLING IN INDUSTRIAL SOLAR SYSTEMS

Hélène DEMASLES^(a), Anouk MULLER^(a), Hai Trieu PHAN^{*(a)}

^(a) Univ. Grenoble Alpes, CEA, Liten, Campus Ines, 73375 Le Bourget du Lac, France

*Haitrieu.PHAN@cea.fr

ABSTRACT

Solar Heat for Industrial Processes (SHIP) is a growing-interest concept in the context of the reduction of both energy consumption and greenhouse gases emissions. As industry often needs cooling power at negative temperatures, solar-fueled NH₃/H₂O absorption systems can be used for this task. In the context of the FriendSHIP European project, a novel design of absorption chiller is investigated for cooling production at -20°C and -40°C from 100-250°C solar heat, based on a GAX (Generator-Absorber heat eXchange) cycle with Plate Heat Exchangers (PHE). This innovative architecture can improve the heat and mass transfers and thus the performance compared to the standard single-stage cycle. In addition, manufacturing costs decrease, as the needed components are standardized and available on the market. As a demonstration, a prototype is built and tested with a target of cold production at -20°C. The experimental data are analysed to give insight for further improvements of the machine.

Keywords: Refrigeration, Ammonia, Absorption, GAX, Solar Heat

1. INTRODUCTION

The efficient use of solar heat and waste process heat is a key point to succeed in the energy transition, as the reduction of energy consumption and the sustainable energy production are fundamental goals that must be aimed to. The SHIP concept (Solar Heat for Industrial Processes) goes in this direction, aiming to provide high-temperature heat to industry by integrating thermal solar and efficient energy storage technologies. However, the need of cooling power is another relevant aspect for many industrial processes, which currently are operated with electric (vapour compression) chillers.

The FriendSHIP European project (Forthcoming Research and Industry for European and National Development of SHIP) addresses this aspect, as one of the goals is to provide both cooling and heating power through the same system. Firstly, a heat carrier fluid is heated up to 200°C-300°C thanks to a combination of different solar technologies (Parabolic Trough Concentrator, Linear Fresnel Receiver) and innovative, high-temperature heat pumps. Then, it can be directly used in industrial processes or stored. The novelty in the system compared to Sharma *et al.* (2017) or Soteris (2003) SHIP architectures is the integration of an absorption chiller, fed with the heat carrying fluid and able to deliver cooling power down to -20°C. This makes the SHIP system less dependent from electric-driven chillers when solar energy is available. Moreover, the absorption chiller can also be fed by the waste heat coming from the rest of the plant. Such a feature increases the energy saving, but requires an absorption chiller able to work effectively with variable heat source temperatures.

Up to now, absorption systems have not been investigated for deep negative cooling purposes. Erikson and Tang (1993) studied a real case application for -15°C cooling, but only for one kind of two-stage cycles. Considering the -20°C or -40°C cooling cases, there is a substantial lack of data about any cycle. A GAX cycle absorption cooling technology in SHIP systems must be interesting due to its large temperature overlap between the generator and absorber, which enables the recovery of a part of the absorption heat release for further vapour generation and thus improve the global performance. A new GAX

prototype was designed, built and tested with the target of cold production at -20°C . This prototype is presented in this work.

2. CYCLE DESCRIPTION

Fluids used in this absorption chiller are $\text{NH}_3/\text{H}_2\text{O}$ where the refrigerant (NH_3) is compatible with the production of sub-zero cold. Heat exchangers of the GAX heat pump are commercial welded plate exchangers chosen for their compactness and thermal performance. The architecture of the GAX chiller is shown in Figure 1.

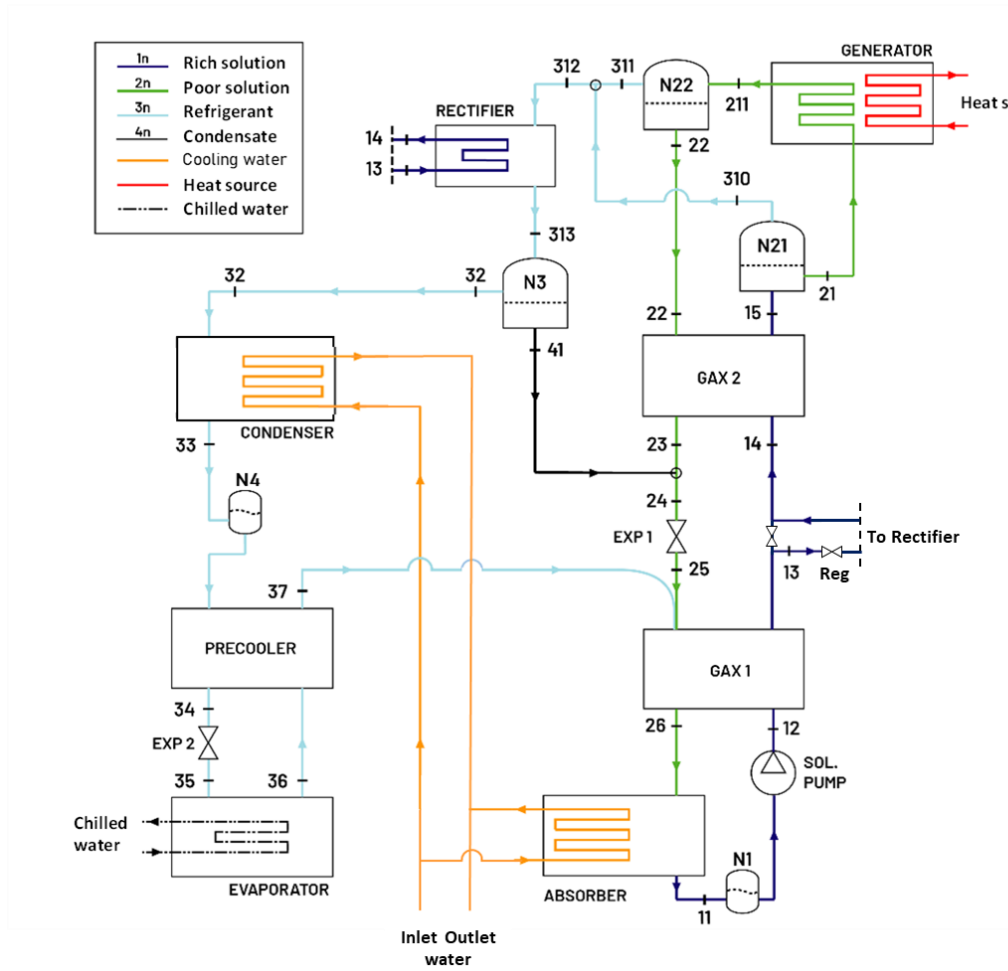


Figure 1: Scheme of GAX prototype architecture

For a convenient description, the chiller cycle can be divided into three subcycles according to the different fluids: refrigerant, rich solution and poor solution.

2.1. Refrigerant subcycle

Due to low difference in the saturation pressures between water and ammonia, some water is desorbed with ammonia during desorption process. To purify the refrigerant, this vapour goes to the rectifier where a beginning of condensation increases refrigerant ammonia concentration. The tank N3 separates purified vapour of condensates that recirculates to the poor solution line. The purified refrigerant is firstly condensed, then subcooled in the precooler before throttling, and finally vaporized in evaporator. After that, the vapour refrigerant is cold in the low-pressure side of the precooler and injected in the GAX1 to be absorbed by the poor solution.

2.2. Rich solution subcycle

The rich solution is brought to a high pressure via a pump before being heated subsequently in GAX1, in rectifier, in GAX2 and then by an external source in the generator. In the first heat exchangers, the solution is heated until reaching saturation temperature. Above this temperature, the desorption starts. To separate the vapour refrigerant of the solution a first separation tank is placed after the GAX1 and a second after the generator. These cascade heat exchangers make it possible to recover as much energy as possible inside the machine and use external energy just to finalize desorption.

2.3. Poor solution subcycle

The liquid poor solution comes out from the bottom of the tank N22 and then it is cooled in the GAX2. Condensates of the rectification are mixed with this solution and the resulting solution is throttled. At the GAX1 inlet, it is mixed with ammonia. The absorption reaction occurs in two heat exchangers : it starts in the GAX 1 using internal cycle energy and ends in the absorber with a colder external source.

3. MODELLING APPROACH

To determine the most efficient solution for the novel GAX ammonia-water cycle, many architectures have been modelled and then implemented in the software EES (Engineer Equation Solver, <http://www.fchart.com/>) to be numerically studied. EES internally provides NH₃/H₂O mixture thermodynamic properties, which are calculated through the correlations proposed by Ibrahim and Klein (1993). The model is established considering each component as a control volume, thus is OD: the internal dynamics are excluded from the study, as the behaviour of each component is considered as a whole and included with a relative efficiency. Even if simple, this approach is reliable for the scope, as it has been largely demonstrated by Herold *et al.* (1996).

For each control volume, mass and energy conservation equations have been defined:

$$\sum \dot{M}_{in} - \sum \dot{M}_{out} = 0 \quad \text{Eq. 1}$$

$$\sum \dot{M}_{in} x_{in} - \sum \dot{M}_{out} x_{out} = 0 \quad \text{Eq. 2}$$

$$\sum \dot{M}_{in} h_{in} - \sum \dot{M}_{out} h_{out} + \sum \dot{Q} - \sum \dot{W} = 0 \quad \text{Eq. 3}$$

In the last equation, \dot{Q} and \dot{W} are the heat and work fluxes exiting the system boundary. Signs respect the traditional convention.

A mass transfer efficiency is applied in heat exchangers where absorption or desorption occurs. This efficiency is the ratio between inlet/outlet concentration differences with the optimal one:

$$\eta = \frac{x_{in} - x_{out}}{x_{in} - x_{out,sat}} \quad \text{Eq. 4}$$

With $x_{out,sat}$ the saturated NH₃/H₂O concentration at temperature and pressure outlet.

Finally, the thermal Coefficient Of Performance (COP) of the chiller is defined as the ratio between the cold produced at evaporator and the energy input in the generator.

$$COP = \frac{\text{useful energy}}{\text{heat cost}} = \frac{Q_E}{Q_G} \quad \text{Eq. 5}$$

4. EXPERIMENTAL SYSTEM

4.1. Prototype

The sizing conditions are reported in Table 1. The generator inlet temperature is set at 130°C, corresponding to the optimal numerical COP. The target of the machine is to produce cold water at -20°C from a lower-temperature heat source (~ 20°C) with a maximum output of 10 kW from positive to negative cold.

Table 1: Prototype nominal point

Parameters	Value	Measure Unit
Generator inlet temperature	130	°C
Absorber inlet temperature	20	°C
Min/Max Evaporator outlet temperature	-20/5	°C
Maximum output	10	kW

Using these values as model inputs, the characteristic parameters of the components are defined. Then, each element is identified on the market, purchased and assembled. To respect the technological readiness asset, only industrial brazed/welded plates heat exchangers are implemented, as those last components are standardized and produced in series. On the contrary, separation and storage tanks, even if they are usual industrial elements, must be designed and singularly manufactured to fit the operating conditions. In addition, as the ammonia/water mixture is very corrosive, a special attention is payed to selecting only resistant components, mostly made of stainless steel. The pressurized tanks and the piping make up the largest share of the material costs of the assembly (without instrumentation) with respectively 36% and 25%, while the plate heat exchangers only represent a smaller share (13%). 3D-view picture of the prototype is shown in Figure 2.

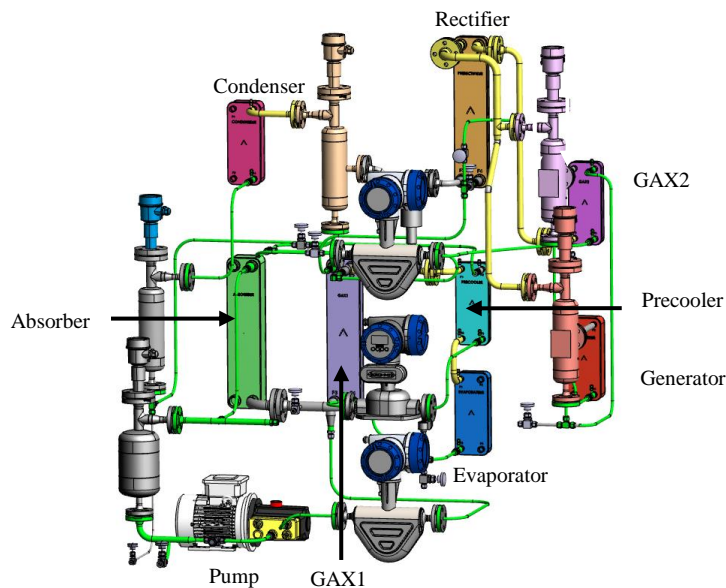


Figure 2: 3D view of the GAX prototype

Three stainless steel tanks are used to separate refrigerant vapour and liquid solution at the outlets of the generator, GAX2 and rectifier. Two other tanks are provided as fluid storages: one to store the poor solution before pumping, in order to avoid pump cavitation during the start-up phase; the other one to store the refrigerant after the condenser. These two storage tanks allow the heat pump to be operated over a wider temperature range. However, the system is filled with relatively low quantities of water and ammonia, 4.5 kg of water and 3.8 kg of ammonia. Finally, the GAX1 heat exchanger features an original, double distributor system for the poor solution and refrigerant inlet, allowing liquid and gas flows to be uniformly distributed into each channel.

4.2. Measurements

Experimental tests were performed at the INES (French National Institute for Solar Energy) facility in a test rig that allows providing adjustable temperatures and powers for the external fluids. The operating field during the tests is reported in Table 2.

Table 2: GAX operating range during experimental test

		Evaporator	Absorber	Condenser	Generator	Pump
Inlet temperature [°C]	Nominal	-20	20	20	130	
	Minimal	-20	15	15	110	
	Maximal	0	25	25	150	
Mass flow rate [kg/h]	External circuits	2600	3500	2700	1200	
Mass flow rate [kg/h]	Internal					170

The prototype is instrumented with high-precision sensors for regulation purposes and for further analysis. Temperature sensors are positioned on the heat exchangers inlets and outlets. The measure of overheating at evaporator outlet is used to regulate the expander opening (EXP 2). Pressure sensors (absolute) are positioned on the high- and low-pressure solution and refrigerant circuits. Coriolis flowmeters are employed to measure mass flow, density and temperature of the solution and refrigerant. Liquid level sensors are placed inside the pressurized tanks to measure the amount of the stocked liquid, thus describing the fluid distribution in the prototype. The level sensor in the separation tank (N22) is used to regulate the opening of the solution valve (EXP 1) and the level sensor in the storage tank upstream the pump (N1) has a protection function, as it shuts off the pump when the stocked liquid level is too low.

Type and uncertainty of the instrumentation are described in Table 3.

Table 3: Instrumentation characteristics

Parameters	Sensors type	Quantity	Uncertainty (+/-)
Heat transfer fluid temperature	Pt100	8	0.1 K
Refrigerant/Solution temperatures	Thermocouples	25	0.3 K
Refrigerant/Solution pressure	0-10 bar and 0-40 bar	4	0.2% full scale
Refrigerant/Solution flow	Mass flowmeter	3	0.20%
External fluid flow	Mass flowmeter	4	0.30%
Density	Mass flowmeter	3	2 kg/m ³
Liquid level	Capacitance level sensor	3	0.50%

The heat flux is calculated on the external side of the heat exchangers (absorber, generator, condenser and evaporator). As an example, the cold output, which is the evaporater power, is defined as:

$$Q_E = \dot{M}_E c_{p,w} (T_{E,in} - T_{E,out}) \quad \text{Eq. 6}$$

where $c_{p,w}$ is the specific heat of water and \dot{M} is the heat carrier fluid flow.

Ammonia fractions are calculated from measured density, temperature and pressure through reverse correlations based on Ibrahim and Klein (1993). Density is measured at three points in order to know the refrigerant concentration after rectification, rich solution concentration at the absorber exit and poor solution concentration at the generator exit. The maximum error is $\pm 2.5\%$.

5. EXPERIMENTAL RESULTS

5.1. Startup

The solution pump starts with an acceleration ramp and its rotation speed is set to reach the nominal rich-solution mass flow rate. Both expander valves (EXP1 and EXP2) are regulated by an automatic control

system. The valve EXP1 is used to regulate the liquid level in the tank N1 in order to avoid cavitation at the pump inlet. The valve EXP2 is set to impose an overheating of the vapour at evaporator outlet of about 3-5 °C. The ratio of the rich solution used for rectification is regulated by measurement of refrigeration temperature at point 313.

As shown in Figure 3, the machine lowers the evaporation temperature until the desired -20°C is reached. This time needed for a stabilized cold production mainly depends on the hydraulic dynamic of the cycle, particularly on the stabilization of the high and low pressures (absolute values). These two pressures are driven by the control parameters such as the pump flow rate and the expansion valves (EXP1 & EXP2) as well as the thermal inertia of the heat exchangers.

During the starting period, we observe that the COP reaches a maximum value of about 0.54 while the cold temperature approaches 0°C and then becomes negative. It is stabilized at a value of 0.35 when the cold temperature reaches -20°C.

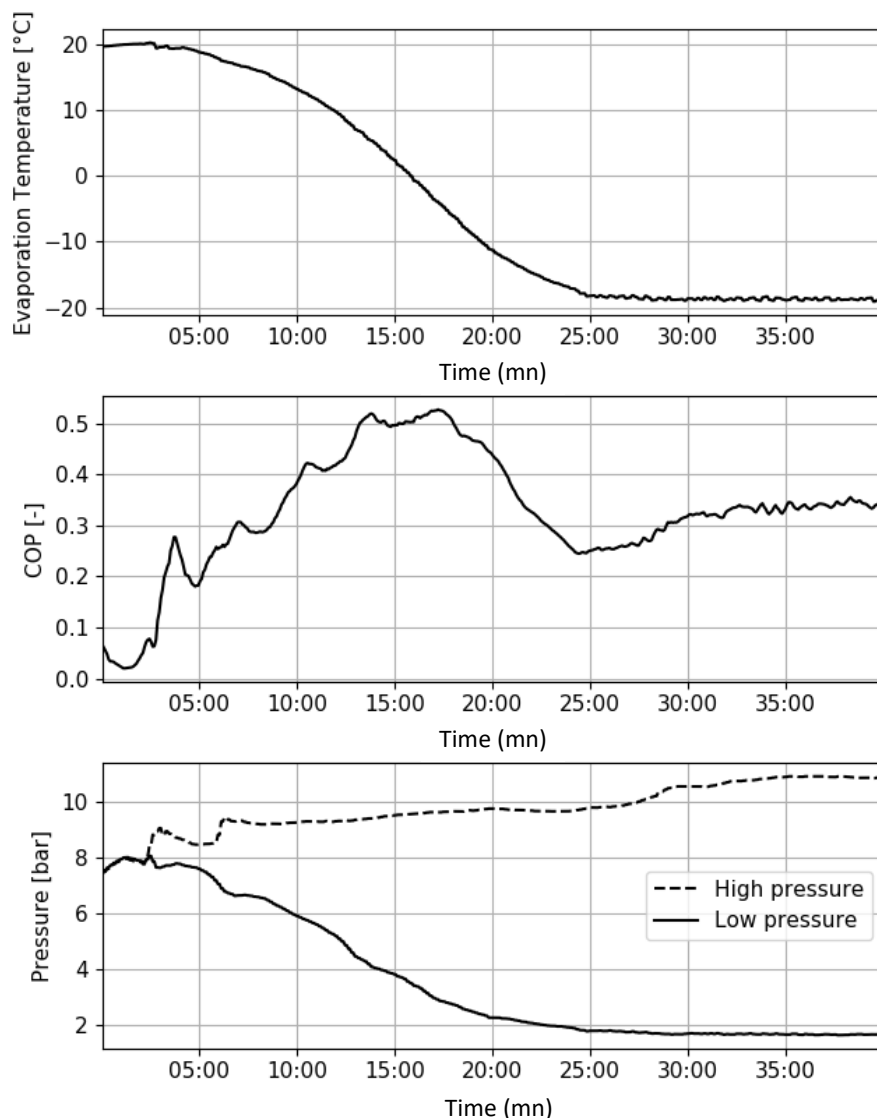


Figure 3 : Evolutions of different parameters during the start-up of the prototype.

5.2. Stabilized performance

The impact of different parameters on the system performance were evaluated. In particular, the study concerns the influences of the generator, evaporator and cooling temperatures (absorber/condenser) and the impact of the rectification. The experimental test conditions were reported in Table 2. For each operating condition, several points were made to ensure measurement repeatability. In the figures

presented below, these points were averaged for greater readability. The dispersion of the points is negligible.

5.2.1. Temperatures variation impact

- Evaporator temperature variation

Figure 4 shows the prototype performances as a function of the evaporator temperature. At -5°C, the prototype provides nearly 11 kW of chilled water with a thermal COP of 0.54. As expected, the performances drop with the evaporator temperature: at -20°C, 6 kW is produced with a COP around 0.36.

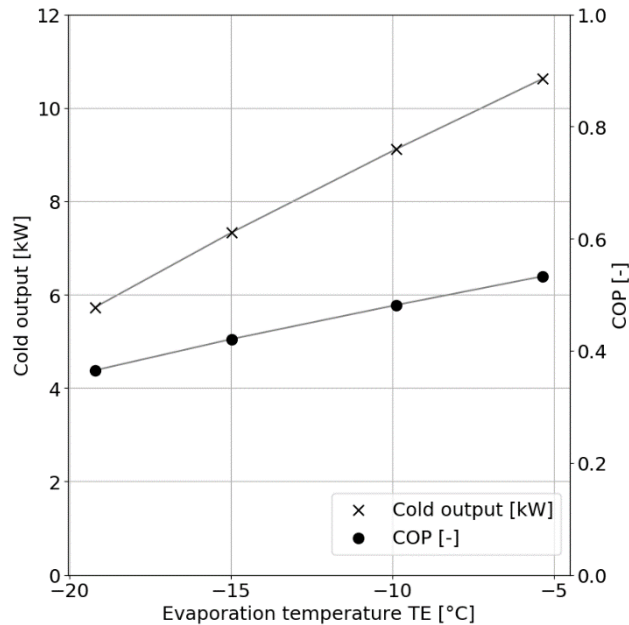


Figure 4 : Evaporator temperature variation impact on cold production and COP with $T_G=120^\circ\text{C}$, $T_A=20^\circ\text{C}$ and $\dot{M}_{pump}=180\text{ kg/h}$

- Generator temperature variation

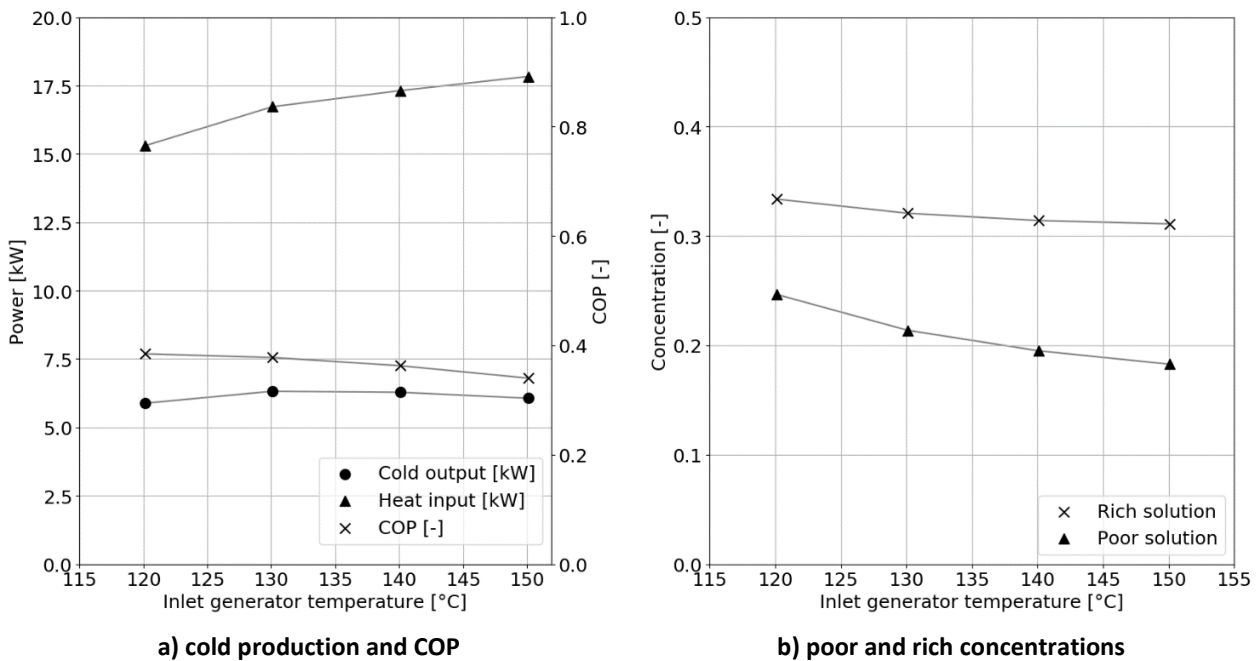


Figure 5 : Generator temperature variation impact with $T_E=-20^\circ\text{C}$, $T_A=20^\circ\text{C}$ and $\dot{M}_{pump}=170\text{ kg/h}$

As shown in Figure 5, increasing the generator inlet temperature results in a slight decrease of the thermal COP while there are an optimal temperature between 130 and 140°C for cold production (a). Indeed, when T_G increases, more vapour is produced at the generator outlet due to a greater desorption (b) but with a higher water content. Therefore, to keep the same refrigerant concentration it is necessary to rectify more and to remove more condensates. The refrigerant flow rate stagnates and no more cold power is produced. However, contrary to the simple-stage simple-effect architecture which presents a sharpen decrease of the COP over the generator temperature, the GAX architecture enables a near flat COP curve and therefore more flexibility of the machine in order to adapt the heat source temperature.

5.2.2. Refrigerant concentration impact

Several rectification temperatures were tested (T_{313}) in order to modify refrigerant quality. As shown on Figure 6, rectification temperature varies between 70 and 86°C. As expected, the refrigerant quality improves when the rectification temperature decreases. An optimal COP is observed for a quality of around 0.975, showing that it is not useful to have too pure ammonia refrigerant: until 0.975, quality improvement allows to produce more cold power with the same evaporator overheating; beyond this, the loss of condensates during rectification leads to an excessive reduction of the refrigerant mass flow rate, decreasing the cold power production.

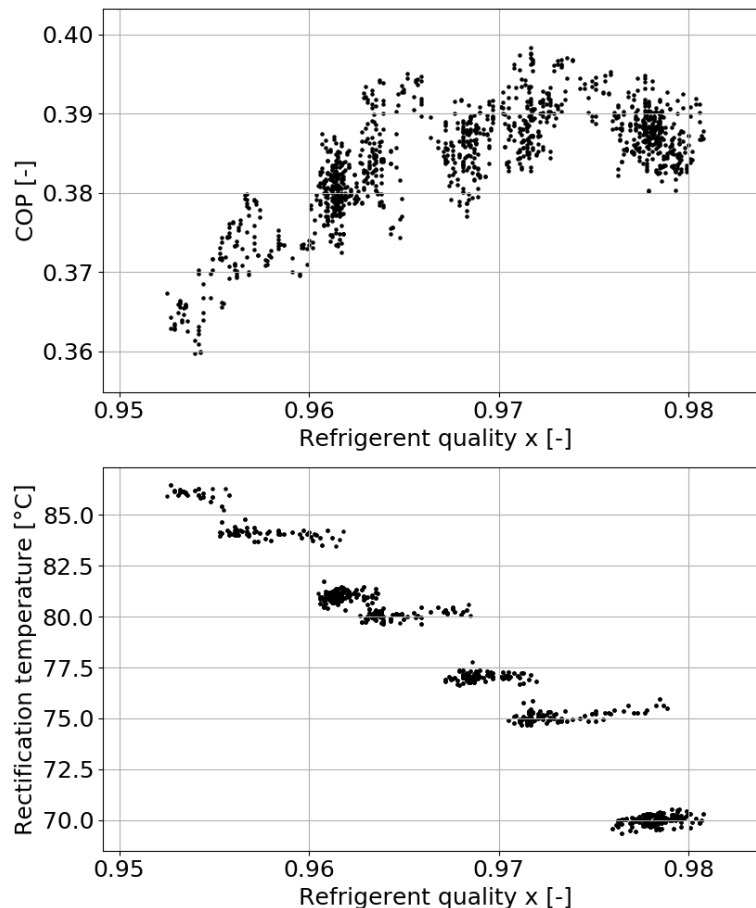


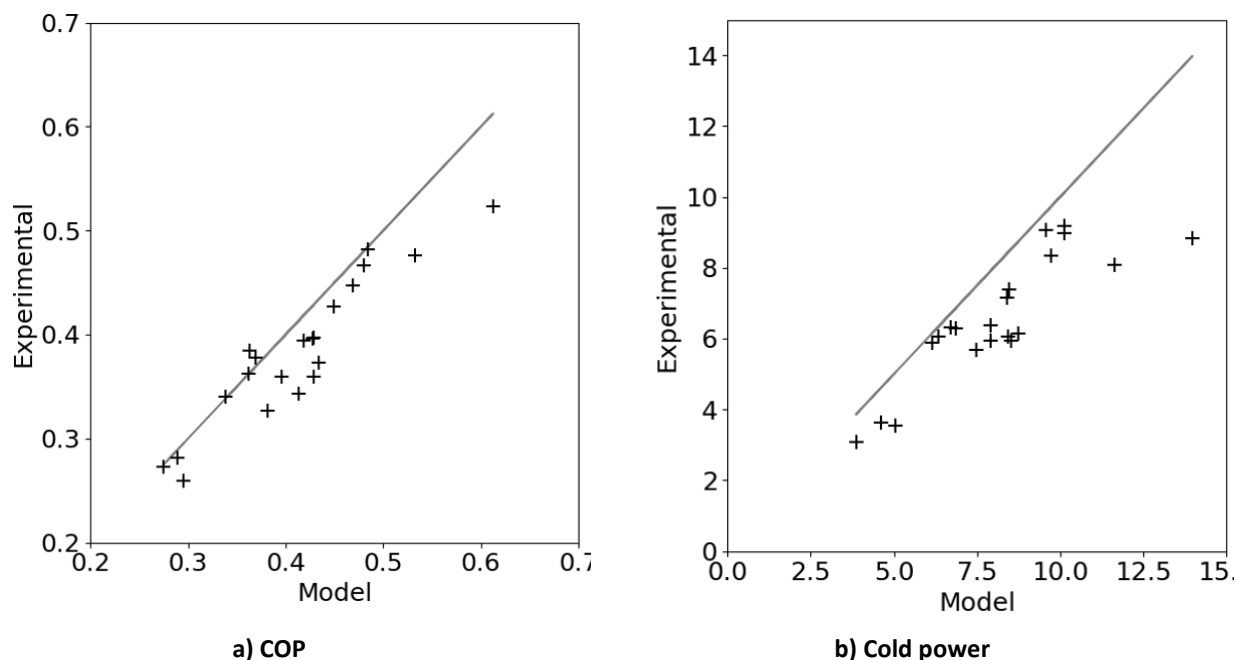
Figure 6 : Rectification temperature impact on refrigerant quality and on the COP

5.3. Comparison of experimental and numerical results

The Figure 7 shows all the experimental stabilized points made under different temperature conditions which are compared to the numerical ones obtained in the same conditions. The temperature ranges tested (T_G , $T_{A/C}$, T_E) vary between ([120;150]°C, [15;25]°C, [0;-20]°C). By specifying the heat and mass efficiencies of the components and integrating the hypothesis listed in Table 4, the model returns the thermodynamic conditions of the state points of the cycle and the global GAX prototype performances.

Table 4: Hypothesis of the model for the prototype modelling

The system is at steady state;	Adiabatic components and pipes;
Pressure drops are negligible;	Ideal heat sources and sinks;
Saturated fluid at separation tanks outlet;	Pump has $\eta_{el} = 0.9$ and $\eta_m = 0.8$;
Evaporator temperature glide is 5°C;	The heat transfer efficiency is 0.8;
	Absorption efficiency is 0.6 and desorption efficiency is 0.4

**Figure 7 : Numerical and experimental results comparison of COP and cold power with $\dot{M}_{pump}=170$ kg/h**

The adjustment of these heat exchangers efficiencies makes it possible to have results presenting the same tendencies with however a slight difference in performance: around 6% and 20% for the COP and the cold power respectively. These comparisons with the model highlight the points to be improved on the prototype. Indeed plate heat exchangers provide satisfying heat transfer but the species mass transfers inside the absorber and the generator remain limited. Future investigations will be carried out in order to improve the distribution of fluids and the time of contact between species in these heat exchangers.

CONCLUSION

This paper presents a new architecture GAX NH₃-H₂O absorption chiller designed with plate heat exchangers in order to offer a compact, easy-to-manufacture machine. An innovative architecture was proposed with the particularity of using internal heat exchangers to enhance energy recovery and minimize external heating. A model was developed for design and preliminary performance simulations. A prototype was built for cold production from 5°C to -20°C. Once the values of the regulation parameters are identified, the start-up of the machine can be easily operated. At -5°C, the prototype provides nearly 11 kW of chilled water with a thermal COP of 0.54. At -20°C, 6 kW is produced with a COP of around 0.36. The tests show the capacity of the machine to operate in a wide range, especially in terms of the inlet temperature of the generator from 120°C to 150°C, which is interesting to address different applications with a flexibility in terms of heat source temperature.

ACKNOWLEDGEMENTS

This project has received funding from the European Union's Horizon 2020 research and innovation programme under grant agreement No 884213, FRIENDSHIP.

NOMENCLATURE

C_p	Specific heat	[J/kg.K]	<i>Subscripts</i>	
\dot{M}	Mass flow	[kg/s]	A	Absorber
η	Efficiency	[-]	C	Condenser
Q	Heat exchange rate	[W]	el	electric
T	Temperature	[K]	E	Evaporator
\dot{W}	Pump work	[W]	G	Generator
x	Ammonia concentration	[-]	in	input
			m	mechanical
			out	output
			sat	saturation
			w	water
<i>Acronyms</i>				
COP	Thermal coefficient of performance			
Exp1	Solution valve			
Exp2	Refrigerant expander			
N	Tank liquid level			

REFERENCES

- Erickson, D.C., Tang, J., 1996. Evaluation of Double-lift Cycles for Waste Heat Powered Refrigeration. ISHPC, Montreal, Canada, pp. 161-168.
- Herold, K. E., Radermacher, R., Klein, S. A., 2016. Absorption chillers and heat pumps, 2nd edition. CRC Press.
- Ibrahim, O.M., Klein, S.A., 1993. Thermodynamic Properties of Ammonia-Water Mixtures. ASHRAE Trans.: Symposia, Vol. 99 (1), pp. 1495-1502.
- Sharma, A. K., Sharma, C., Mullick, S.C., and Kandpal, T.C., 2017. Solar industrial process heating: A review. Renewable and Sustainable Energy Reviews, 78, 124-137.
- Soteris, K., 2003. The potential of solar industrial process heat applications, Applied Energy, 76, 337-361.